Factorial moments of continuous order

Rudolph C. Hwa
Institute of Theoretical Science and Department of Physics, University of Oregon, Eugene, Oregon 97403
(Received 3 November 1994)

The normalized factorial moments F_q are continued to noninteger values of the order q, satisfying the condition that the statistical fluctuations remain filtered out. That is, for the Poisson distribution $F_q = 1$ for all q. The continuation procedure is designed with phenomenology and data analysis in mind. Examples are given to show how F_q can be obtained for positive and negative values of q. With q being continuous, a multifractal analysis is made possible for multiplicity distributions that arise from self-similar dynamics. A step-by-step procedure of the method is summarized in the conclusion.

PACS number(s): 13.85.Hd, 25.75.+r

I. INTRODUCTION

Continuation of the normalized factorial moments F_q to arbitrary, noninteger values of q is not just a mathematical problem. It has high phenomenological significance, and provides a powerful method to analyze experimental data that can reveal aspects about multiplicity fluctuations hitherto unexplored.

A historical review of the problem is in order. Bialas and Peschanski [1] first introduced F_q as a means of studying the scaling behavior of multiplicity fluctuations as a function of the resolution scale δ, a subject usually referred to as intermittency. Although a large part of the effect seen in the data has recently been found to be due to Bose-Einstein correlation among like-charge particles [2,3], intermittency at a weaker level is still present for the unlike-charge particles and its origin remains to be clarified [4], especially for $q > 2$. There is far more dynamical information about high-energy collisions than can be uncovered by studying two-particle correlation only. With that point of view forming the basis of our discussion here, we now outline the problems associated with the use of F_q.

Let us first recall the definition of F_q:

$$F_q = \frac{\langle n(n-1)\cdots(n-q+1)\rangle}{\langle n\rangle^q} , \quad (1)$$

where angular brackets denote an average weighted by the multiplicity distribution P_n. The most outstanding property of F_q discovered in Ref. [1] is that it filters out the statistical fluctuations, so any nontrivial behavior of F_q is a direct indication of some features about the dynamics of particle production. A quick review of that will be given in the beginning of the next section. Another significant aspect about F_q is that an event can contribute to (1) only if $n \geq q$. Thus for small δ where $\langle n\rangle$ is small in a bin, only rare events with high spikes ($n \geq q$) contribute. That is why it is sometimes said that intermittency measures spiky events. There are, however, disadvantages in the use of F_q. A corollary to the ability to select spiky events is its inability to extract any dynamical information about dips. It is by now generally recognized that rapidity gaps, like voids in galactic structure, are important to study. Those are, of course, large dips. In nuclear collisions where multiplicity per bin is large, unusual dips, which can be small but deep, are as significant as unusual spikes. For such fluctuations it is necessary to study F_q for $q < 1$, especially negative q. Furthermore, for multifractal analysis of multiparticle production the continuation of F_q to noninteger values of q is necessary in order to allow differentiation with respective to q. These studies cannot be done, if F_q is defined as in (1).

A method to investigate moments of arbitrary order was suggested several years ago in terms of the G moments [5]. It was later modified to achieve better power-law behavior [6]. However, in overcoming the defects of F_q, the G moments fail to retain the principal attribute of F_q, i.e., the screening of statistical fluctuations. Subtraction of the statistical component has to be done by hand [7]. Since that can be achieved only by simulation, the method is not elegant. But it has provided the first glimpses into the multifractal structure of particle production.

In this paper we describe a method that retains both attributes: it eliminates statistical fluctuations and is defined for continuous q. Although the mathematical technicalities involved may at first sight appear to be of theoretical interest only, the method is developed with phenomenology in mind. The purpose of the program is to extract quantitative information about dynamical fluctuations from the experimental data and to present it in a form suitable for comparison with theoretical predictions. Thus the problem of data analysis has not been overlooked in favor of mathematical expediency in the hope that the procedure can be readily accessible to direct experimental application.

II. THE PROBLEM

We first review the virtue of factorial moments. To say that F_q filters out statistical fluctuation, one first assumes that the latter enters the multiplicity distribution as a convolution with the dynamical component

$$P_n = S \otimes D \ , \tag{2}$$

where S represents the statistical component, which we take to be the Poisson distribution $\mathcal{P}_n^{(0)}$, and D is the dynamical distribution. More specifically, (2) implies

$$P_n = \int_0^\infty dt \frac{t^n}{n!} e^{-t} D(t) \ . \tag{3}$$

Let the numerator of (1) be denoted by f_q, i.e.,

$$f_q = \sum_{n=q}^{\infty} \frac{n!}{(n-q)!} P_n \ , \tag{4}$$

which is well defined for q being a positive integer. Substituting (3) in (4) and performing the summation yields

$$f_q = \int_0^\infty dt\, t^q D(t) \ . \tag{5}$$

This is the qth moment of the dynamical $D(t)$ and is free of statistical contamination. Since $f_1 = \langle n \rangle$, we have

$$F_q = f_q / f_1^q \ . \tag{6}$$

If P_n is a Poisson distribution, then $D(t) = \delta(t - \langle n \rangle)$ and $f_q = \langle n \rangle^q$ so

$$F_q = 1 \ \text{ for integer } q \geq 1 \ . \tag{7}$$

Because of this trivial result, one can state that any nontrivial F_q reveals the nontrivial properties of $D(t)$.

To generalize F_q to noninteger q, it must first be recognized that there is no unique continuation to complex q. Since P_n must vanish as $n \to \infty$ (in fact, it must vanish for $n > N$ for some finite N at any finite collision energy), there are only a finite number of the F_q moments defined at integer q values. Without an accumulation of F_q at infinite q, unique continuation to noninteger q is not possible. Put differently, we can add to F_q any arbitrary function that vanishes at the finite range of integer q where F_q is specified and generate another function F_q at noninteger q.

A simple way of continuing (4) to arbitrary q is to replace the factorial by Γ functions: i.e.,

$$f_q = \sum_{n=0}^{\infty} \frac{\Gamma(n+1)}{\Gamma(n-q+1)} P_n \ . \tag{8}$$

Procedures similar to (8), such as continuing $d^q G(z)/dz^q$ to fractional q [8], have been considered previously [9–11]. Since $\Gamma(z)$ has poles and oscillates rapidly among those poles when $z \leq 0$, F_q as defined in [8] oscillates between large positive integers of q and is highly suppressed at large negative q. The question is whether one wants that kind of behavior at noninteger values of q. If not, what are the guidelines by which one makes alternative choices of the continuation schemes?

In our view the only guideline is the primary rationale for considering factorial moments in the first place. And that is the elimination of statistical fluctuation at all q, not just at integer values of q. If one substitutes Poisson distribution into (8), one will find that $f_q \neq \langle n \rangle^q$. Figures 1(a) and 1(b) show the results for F_q when

$$P_n = \mathcal{P}_n^{(0)} = \frac{\langle n \rangle^n}{n!} e^{-\langle n \rangle} \ , \tag{9}$$

for $\langle n \rangle = 6$. Although (7) remains true for positive integers of q, F_q is by no means equal to one for all q. The oscillations have larger amplitudes at high q, as revealed in Fig. 1(b). The situation is worse at smaller $\langle n \rangle$. In Fig. 2, we show the result for $\langle n \rangle = 1$ in (9), for which

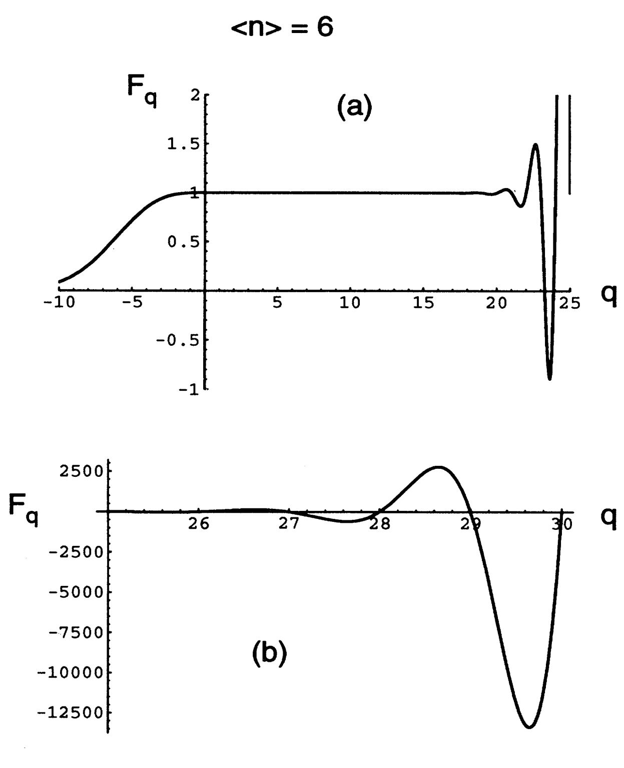

FIG. 1. Normalized factorial moments F_q in the simple continuation procedure using (8) with Poisson distribution (9) as input and with $\langle n \rangle = 6$. (a) $-10 \leq q \leq 25$; (b) $25 \leq q \leq 30$.

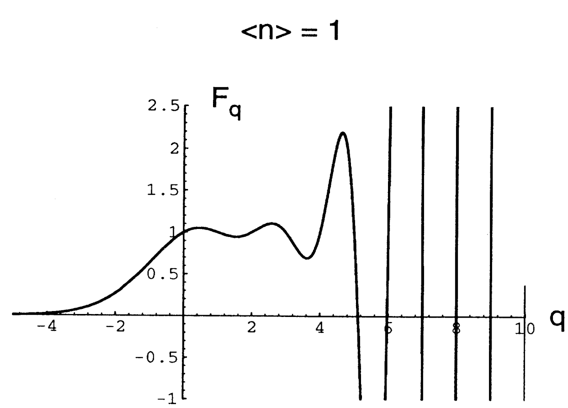

FIG. 2. Same as Fig. 1 but for $\langle n \rangle = 1$.

(6) and (8) are again used. Notice that there is no connected region of q in which $F_q = 1$, not even between $q = 1$ and 2. Between $q = 9$ and 10 the peak of $|F_q|$ is greater than 10^4. From these results it is therefore not possible to claim that (8) contains no statistical contribution at noninteger q. The reason for studying F_q at noninteger q is consequently lost. The G_q moments [5,6] would be better.

III. THE SOLUTION

To achieve our aim of retaining only the dynamical fluctuation in our continuation procedure, we demand that (5) defines $f(q)$ for all q. Hereafter, we use the notation that when q appears as an argument of a function, instead of as a subscript, it is to be regarded as a continuous (complex) variable. A consequence of that condition is that the normalized factorial moment function satisfies

$$F(q) = 1 \tag{10}$$

for all q in the case of Poisson distribution. Equation (10) should be used as a test of the continuation procedure.

The burden of this procedure is to determine $D(t)$. If a theory specifies the dynamical distribution $D(t)$ completely, then (5) prescribes a unique continuation of f_q to the complex function $f(q)$ at any q. But how is that to be checked by experiments where only P_n is measured? Thus the procedure must supplement (5) with a way of determining $D(t)$ from P_n. This deconvolution process also cannot be made unique. The discrepancies show up as deviations of $F(q)$ from 1. The region where (10) fails significantly can fortunately be controlled and pushed to large $|q|$.

To deconvolute (3) one could consider making the inverse Laplace transform of the generating function $G(z)$. However, there are difficulties connected with the fact that $G(z)$ determined from the experimental P_n is a polynomial having no singularities in the finite z plane.

Our proposal is to expand P_n in terms of negative binomial distributions (NBD's) $P_n^{\rm NB}(j)$. One of the attributes of NBD is that it can also be expressed as a Poisson transform [12], as in (3). They do not form a complete set of orthogonal functions, so in general they cannot be the basis functions for the expansion of an arbitrary function. However, we do not have an arbitrary function. The experimental P_n (ignoring errors for the moment) is a set of $N + 1$ numbers for $n = 0, 1, \ldots, N$. Thus the expansion

$$P_n = \sum_{j=0}^{N} a_j P_n^{\rm NB}(j) \tag{11}$$

is well defined with $N + 1$ coefficients a_j, provided we specify $P_n^{\rm NB}(j)$ appropriately. One could consider other distributions instead of NBD, but for factorial moments that we shall eventually calculate NBD is most convenient.

Now $P_n^{\rm NB}(j)$ is defined by [12]

$$P_n^{\rm NB}(k_j, x_j) = \frac{\Gamma(n + k_j)}{\Gamma(n+1)\Gamma(k_j)} \left(\frac{k_j}{k_j + x_j}\right)^{k_j} \times \left(\frac{x_j}{k_j + x_j}\right)^{n} , \tag{12}$$

where x_j and k_j specify the mean and inverse width of $P_n^{\rm NB}(j)$. How they depend on j will be discussed in the next section. We remark that x_j is equal to

$$\bar{n}(j) = \sum_{n=0}^{\infty} n P_n^{\rm NB}(j) \tag{13}$$

only if the sum extends to ∞ . Since our method is designed with phenomenological analysis in mind, where P_n is given only for $n = 0, \ldots, N$, all sums over n will be from 0 to N, whether the summand involves P_n or $P_n^{\rm NB}$. Consequently, x_j is not *exactly* $\bar{n}(j)$. Although the discrepancy is small for the x_j and k_j to be chosen, accuracy will be important, as we shall see. Extending the sum in (11) to a larger upper limit N' with $P_n = 0$ for $N + 1 \leq n \leq N'$ would cause a_j to be very large and highly sensitive to the accuracy of the calculation; it is a procedure that should be avoided. Hereafter N will always be the maximum value of n for which P_n is measured to be nonzero, and x_j and k_j should only be regarded as real parameters of $P_n^{\rm NB}(j)$ that will be varied in the expansion in (11). It should be recognized that because $P_n^{\rm NB}(j)$ are all positive (unlike a harmonic function) and small on the wings, a_j will have alternating signs and can have large absolute values if P_n is small for a range of large n values. Thus accuracy in the ensuing calculations will be essential. With $P_n^{\rm NB}(j)$ specified, (11) is a set of $N + 1$ simultaneous algebraic equations that can be solved for a_j in terms of the experimental P_n.

Define $D^{\rm NB}(t)$ by the negative-binomial versions of (3), i.e.,

$$P_n^{\rm NB}(j) = \int_0^{\infty} dt \frac{t^n}{n!} e^{-t} D^{\rm NB}(t, j) \ . \tag{14}$$

Then it is known that [12]

$$D^{\rm NB}(t, j) = \left(\frac{k_j}{x_j}\right)^{k_j} \frac{t^{k_j - 1}}{\Gamma(k_j)} e^{-k_j t / x_j} \ . \tag{15}$$

The substitution of (3) and (14) to the two sides of (11) results in

$$D(t) = \sum_{j=0}^{N} a_j D^{\rm NB}(t, j) \ . \tag{16}$$

Thus we have inverted (3) and extracted the dynamical distribution $D(t)$ from the experimental data on P_n. In principal, this $D(t)$ can be compared directly with the theoretical distribution. However, the more familiar arena for comparison involves the factorial moments, which are more closely related to the data.

An interesting side remark that can be made here is that the feasibility of determining $D(t)$ from the data makes possible an experimental look at such theoretical quantity as the Landau free energy if the data on hadronic multiplicity distribution correspond to quark-hadron phase transition [13], or if the data are on photon distribution at the threshold of lasing in quantum optics [14]. That is because in such problems $D(t)$ in (3) is $e^{-F[t]}$, where $F[t]$ is the free energy of the system.

Returning to the problem on the factorial moments, we substitute (16) into our basic equation, (5), for continuation to complex q, and get

$$f(q) = \sum_{j=0}^{N} a_j f^{\rm NB}(q,j) \ , \qquad (17)$$

where

$$f^{\rm NB}(q,j) = \left(\frac{x_j}{k_j}\right)^q \frac{\Gamma(q+k_j)}{\Gamma(k_j)} \ . \qquad (18)$$

This expression is obtained by integration over t in (5) and is valid only for

$$\mathrm{Re}q > -k_j \ . \qquad (19)$$

Thus the domain of q that can be continued into before encountering the first singularity is governed by the smallest value of k_j.

It should be noted that whereas f_q as defined in (4) is obtained directly from the input P_n, $f(q)$ is determined from (17) after the inversion is done and the continuation procedure followed. Even at positive integer values of q, $f(q)$ is not exactly equal f_q because of finite accuracy in the computation. Following (6), we define the continued normalized factorial moments by

$$F(q) = f(q)/f(1)^q \ , \qquad (20)$$

instead of $f(q)/\langle n\rangle^q$. From (17) and (18) we then have

$$F(q) = \sum_{j=0}^{N} a_j \left[\frac{x_j}{f(1)}\right]^q F^{\rm NB}(q,j) \ , \qquad (21)$$

where

$$F^{\rm NB}(q,j) = \frac{\Gamma(q+k_j)}{\Gamma(k_j)k_j^q} \ . \qquad (22)$$

Equation (21) is our result, which is explicit once the values of a_j are determined.

IV. THE RANGE OF x_j AND k_j

To complete the description of our continuation procedure, it is necessary to specify x_j and k_j, which represent the average and inverse width of $P_n^{\rm NB}(j)$. They should be chosen to be not too far from the values of x and k of the input P_n, where

$$x \equiv \langle n\rangle = \sum_{n=0}^{N} nP_n \ , \qquad (23)$$

$$k \equiv (F_2-1)^{-1}, \quad F_2 = \langle n(n-1)\rangle/x^2 \ . \qquad (24)$$

We therefore define first

$$\Delta_j = \Delta\left(-\frac{1}{2}+\frac{j}{N}\right) \ , \qquad (25)$$

which ranges from $-\Delta/2$ to $+\Delta/2$ in equal steps, as j varies from 0 to N. For x_j and k_j to vary from the lower to higher sides of x and k, we set

$$x_j = x(1+\Delta_j) \ , \qquad (26)$$

$$k_j = k(1+\Delta_j) \ . \qquad (27)$$

Thus $P_n^{\rm NB}(j)$ with lower x_j has wider width (lower k_j); while that with higher x_j has narrower width. If Δ is not too large, all components $P_n^{\rm NB}(j)$ will have comparable magnitudes at large n, which should be small where P_n is small. Otherwise, a_j would be hypersensitive to the accuracy of the computation. With Δ being free to choose, the procedure is obviously not unique. As we have remarked earlier, no unique continuation should be expected from a finite set of numbers, P_n. However, there are guidelines for an optimal choice of Δ. If x is very small, then (26) may have to be modified, as discussed in the last paragraph of this section.

We have mentioned in connection with (19) that the domain of continuation of q is limited by the smallest value of k_j, which is $k(1-\Delta/2)$. Thus to increase that domain we would want to have a small value for Δ. However, with a small range of x_j and k_j it will be necessary to have highly accurate expansion coefficients a_j in (11) to well represent P_n. So a larger value of Δ is preferred. This point needs to be demonstrated quantitatively. A way to do this is to calculate $f(1)$ and examine its dependence on Δ. To that end we consider specific examples in the following.

Consider a sample P_n given by

$$\mathcal{P}_n^{(1)} = (n+0.3)^3 e^{-0.5n}/Z, \quad n = 0,\ldots,N \ , \qquad (28)$$

where $N = 30$ and Z is the normalization factor so that $\sum_{n=0}^{N} \mathcal{P}_n^{(1)} = 1$. For this $\mathcal{P}_n^{(1)}$ we have $x = \langle n\rangle = 7.6966$ and $k = 7.2193$. For Δ chosen to be in the range $0.1 \leq \Delta \leq 0.6$, we follow the procedure described in Sec. III and calculate $f(1)$. The result is shown in Fig. 3(a) as a function of Δ. Evidently, there are fluctuations at small values of Δ, but quite stable for $\Delta \geq 0.25$. However, when the vertical scale is expanded as shown in Fig. 3(b), we see that small fluctuations at a level of $< 0.3\%$ are still present until $\Delta \geq 0.4$, where $f(1) = 7.7016$. A discrepancy between $f(1)$ and x is anticipated because of the finiteness of N but at 0.06% level it is unimportant. What is important is that Δ should not be too small. This example demonstrates the limitation of the method due to (19), if one attempts to continue q to large negative values. From Fig. 3 an appropriate value for Δ can be set at 0.5, for which $\min\{k_j\} = 0.75k = 5.4145$. Thus $F(q)$ can be continued to $q \simeq -5.4$ before encountering divergence. In practice this range of negative q is quite

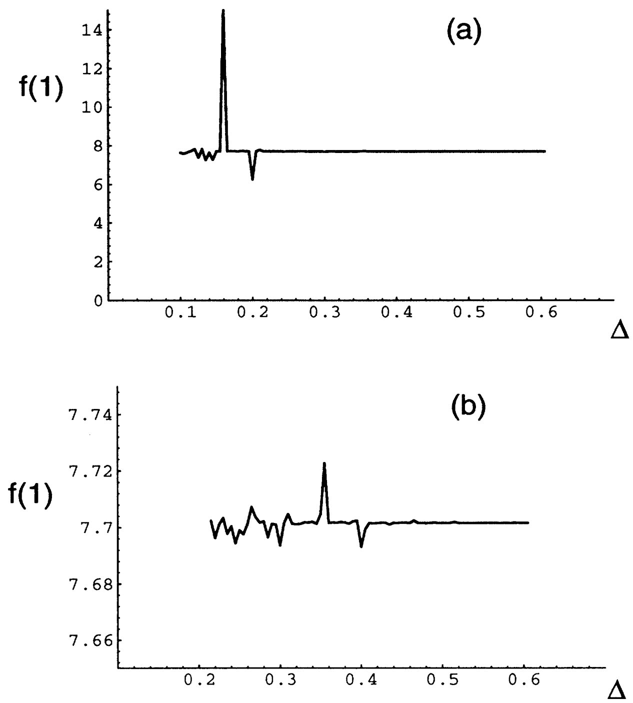

FIG. 3. Dependence of factorial moment $f(q=1)$ on Δ when the input distribution is $\mathcal{P}_n^{(1)}$. The resolution in (b) is higher than that in (a).

enough to exhibit the low-n behavior of P_n. Increasing Δ would improve the stability of the solution, but decrease the range of continued q. The choice of $\Delta = 0.5$ seems like a good compromise between the two opposite preferences.

Consider next another example where $\langle n \rangle$ is much smaller, corresponding to the situation where the phase-space cell size δ is small. Assume

$$\mathcal{P}_n^{(2)} = (n+1)^{0.5} e^{-n}/Z, \quad N = 20 , \tag{29}$$

for which $x = 0.8352$ and $k = 1.395$. Figure 4 shows the result of $f(1)$ vs Δ, which is rather free of fluctuation for all Δ except near 0.1. The value of $f(1) = 0.8352$ is equal to x to 5 significant figures. Choosing $\Delta = 0.5$ gives $\min\{k_j\} = 1.046$ which does not allow q to go much beyond -1. Decreasing Δ would not improve the situation due to the limitation of small k for $\mathcal{P}_n^{(2)}$. Since Δ should not be changed in the analysis of data with varying δ, we suggest that Δ be fixed at 0.5.

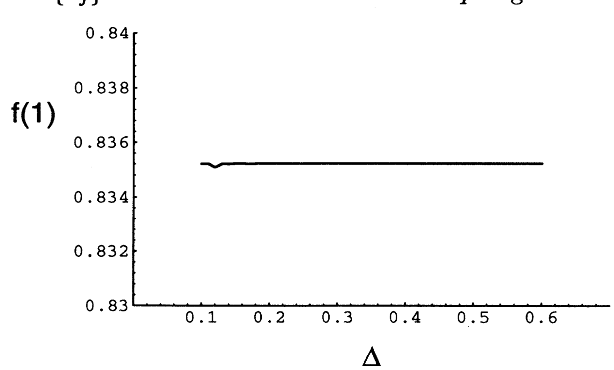

FIG. 4. Dependence of $f(q=1)$ on Δ when the input distribution is $\mathcal{P}_n^{(2)}$.

There are situations where (26) may not be the optimal choice for x_j. Such is the case when x is extremely small, e.g., 0.1, while $N = 5$. Then, x_j varies from 0.05 to 0.15, which does not provide enough range to expand P_n in without demanding extremely high accuracy in the computation. A more suitable definition can be, for example,

$$x_j = 0.01N + 0.09j , \tag{30}$$

which ranges from $N/100$ to $N/10$. We have tried this for some sample distributions and it works very well. In the following only (26) is used, not (30).

V. CONTINUED FACTORIAL MOMENTS

The continuation procedure having been completely specified in Secs. III and IV, we can now proceed to the study of the normalized factorial moments $F(q)$. We continue to use the three distributions $\mathcal{P}_n^{(i)}$, $i = 0, 1, 2$, as our sample inputs for P_n. Unless otherwise stated, $\Delta = 0.5$ is used.

For the Poisson distribution $\mathcal{P}_n^{(0)}$, let us consider the same two cases: (a) $\langle n \rangle = 6$ and (b) $\langle n \rangle = 1$, already examined in Sec. II, where the simple continuation scheme $n! \to \Gamma(n+1)$ was used. Now, we assume $N = 30$ for (a) and $N = 10$ for (b) as the upper limits of n in the experimental P_n. If $N = \infty$, $\mathcal{P}_n^{(0)}$ would give $F_2 = 1$, so according to (24) k would be infinite. For the finite N chosen for the two cases, F_2 are still very close to 1, so k would be extremely large. For our calculation it is sufficient to set $k = 10^4$. Using our procedure of continuation the results are shown in Figs. 5(a) and 5(b), for the two cases (a) and (b), respectively. Note the high resolution of the vertical scale. For $\langle n \rangle = 6$ in case (a) $F(q)$ is essentially 1 for $-10 < q < 30$. In case (b) where $\langle n \rangle = 1$, $F(q)$ is almost 1 for $-10 < q < 20$ except near the edges of that range. This case is more difficult to continue accurately because there are fewer values of nonvanishing $\mathcal{P}_n^{(0)}$. Theoretically, $\mathcal{P}_n^{(0)}$ is nonzero for any finite n, but we cut off at $N = 10$ to simulate a realistic situation where $\langle n \rangle$ is only 1. With only 11 values of a_j the continuation to large $|q|$ cannot be expected to have extremely high accuracy. That is why $F(q)$ deviates from 1 near the two ends in Fig. 5(b). Nevertheless, the deviation is only of order 0.1%. Upon comparing Fig. 5 to Figs. 1 and 2, the advantage of this method over the simple scheme of Sec. II is self-evident.

For $\mathcal{P}_n^{(1)}$ given in (28) with $N = 30$ the result of our calculation for $F(q)$ is shown in Figs. 6(a) and 6(b). The dependence on q is evidently very smooth. It grows rapidly at negative q, even though the first singularity is located at $q < -5$. We have also calculated $F(q)$ for $\Delta = 0.3$, the result of which is plotted in dashed lines, lying very close to the solid lines for $\Delta = 0.5$. For $q > 0$ the

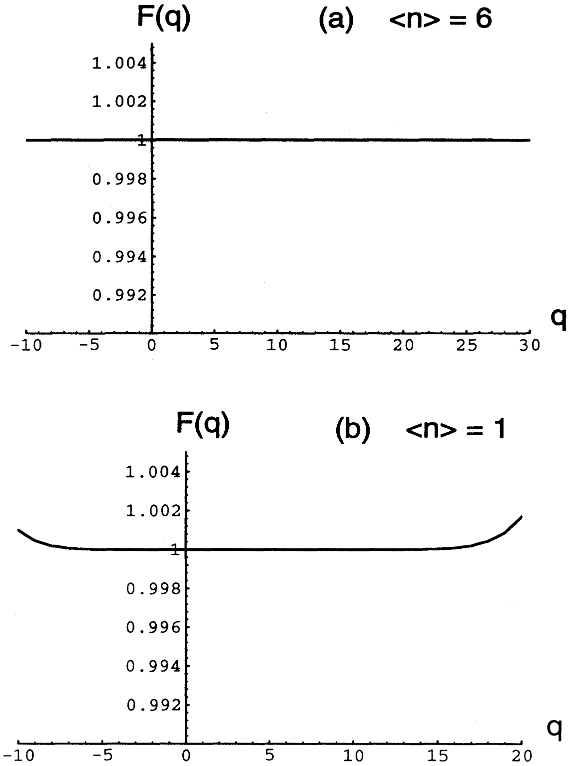

FIG. 5. Normalized factorial moments $F(q)$ with high vertical resolution for Poisson distribution with (a) $\langle n \rangle = 6$ and (b) $\langle n \rangle = 1$.

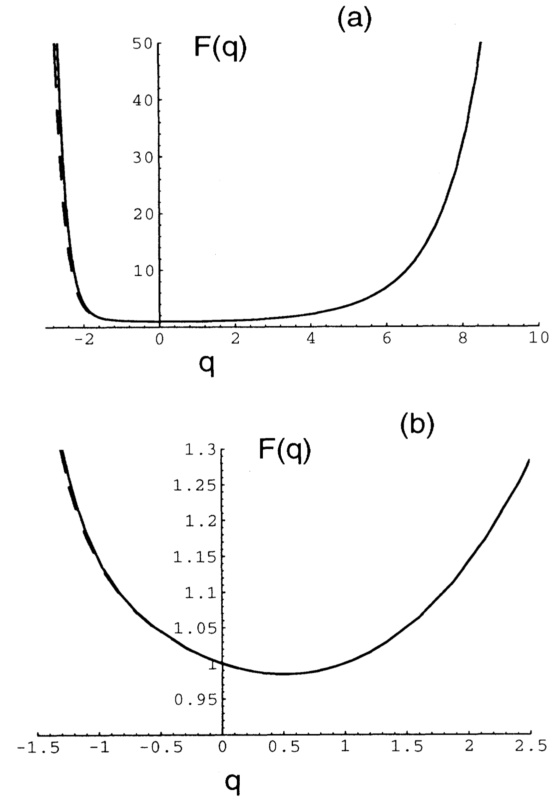

FIG. 6. $F(q)$ with $\mathcal{P}_n^{(1)}$ as input distribution. The solid line is for $\Delta = 0.5$, the dashed line is for $\Delta = 0.3$. (a) $-3 \leq q \leq 10$; (b) $-1.5 \leq q \leq 2.5$.

two cases are indistinguishable. For $q < -2$ the difference is actually not negligible in absolute value but because of the rapid rise of $F(q)$ it is not significant in terms of percentage discrepancy. In Fig. 6(b), we see that for the range of q shown the difference between the two cases is totally insignificant. This is the most important range for the continuous q problem, and we have found a reliable continuation of $F(q)$.

It should be pointed out that $F(0) = 1$ is not accidental. From (21) and (22) we see that $F(0) = \Sigma_j a_j$, which is 1 by virtue of the normalization of P_n and $P_n^{\rm NB}(j)$ in (11). Of course, f_0 is also 1 if the continuation scheme of (8) is followed.

Finally, let us come to the third example where $\mathcal{P}_n^{(2)}$ is as given in (29) with $N = 20$. Now, the values of x and k are small. The calculated result for $F(q)$ is shown in Figs. 7(a) and 7(b). There is a fast rise at large q because of the smaller x (compared to the case above). The continuation to negative q encounters irregularity due to the small value of k. For $q > -0.5$, there is essentially no difference between the use of $\Delta = 0.5$ (solid line) and $\Delta = 0.3$ (dashed line). Only the solid line is plotted in Fig. 7(a); both are plotted in Fig. 7(b). The difference between the two Δ cases becomes noticeable and quantitatively significant only for $q < -0.5$, a region very close to the singularities. The reliability of our continuation should therefore be restricted to the domain to the right of the sudden downturn of $F(q)$ around $q = -0.5$. In that domain our result is smooth and insensitive to Δ.

VI. MULTIFRACTAL ANALYSIS

With $F(q)$ continuable to noninteger q, it is now possible to consider multifractal analysis, assuming that $F(q)$ has a power-law dependence on the resolution scale δ for a range of q covering both positive and negative values. Such an analysis was suggested previously using G moments, which are defined for all q by [5]

$$G(q) = \sum_i \left(\frac{n_i}{n_t} \right)^q , \tag{31}$$

where n_i is the multiplicity in bin i, $n_t = \sum_i n_i$, and the sum in i is over all nonempty bins. $G(q)$ shows scaling behavior

$$G(q) \sim \delta^{\tau(q)} \tag{32}$$

for $q > 1$ in both experimental data and model simulation, when $\theta(n_i - q)$ is included in the summand in (31) [6]. However, for $q < 1$ (32) is not valid for any extended range of δ, so multifractal analysis cannot be made for that range of q. The problem is rooted in the empty-bin effect and the fact that $G(q)$ contains statistical fluctuations. Since $F(q)$ is now defined for noninteger q, its scaling behavior

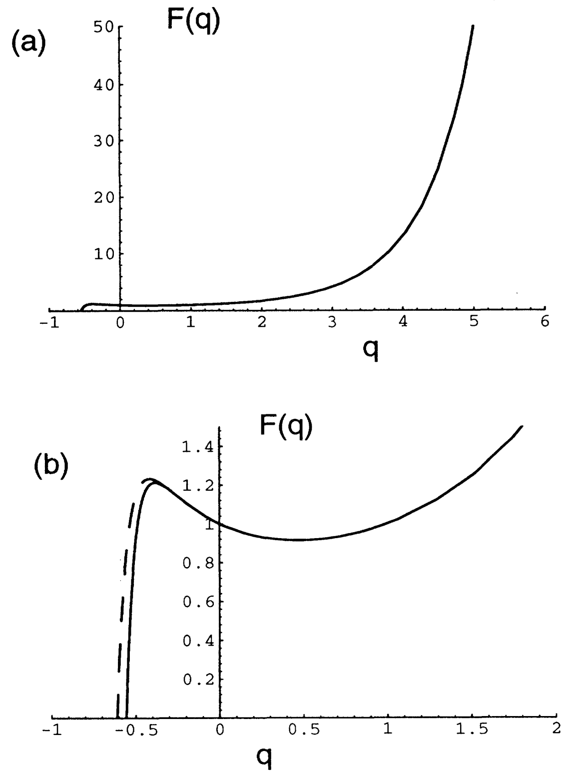

FIG. 7. $F(q)$ with $\mathcal{P}_n^{(2)}$ as input distribution. The solid line is for $\Delta = 0.5$, the dashed line is for $\Delta = 0.3$. (a) $-1 \le q \le 6$; (b) $-1 \le q \le 2$.

$$F(q) \propto \delta^{-\varphi(q)} , \tag{33}$$

especially for negative q, should be checked for a variety of existing data. If (33) is valid for a range of q around 1, multifractal analysis can then proceed without the necessity of subtracting out the statistical component, as was done for $G(q)$.

We can relate $G(q)$ and $F(q)$, if we assume that (31) is defined for the dynamical distribution only without the statistical fluctuation. The sum over all bins in (30) can then be related to averaging over the dynamical distribution in (5). Using (6), (32), and (33), we get

$$\tau(q) = q - 1 - \varphi(q) , \tag{34}$$

where the -1 comes from the fact that $\sum_i$ by itself gives the total number of bins, which varies as δ^{-1}. The multifractal spectrum is then obtained by the Legendre transform [5,15]

$$f(\alpha) = q\alpha - \tau(q) \tag{35}$$

with

$$\alpha = d\tau(q)/dq . \tag{36}$$

Thus the verification of the power law (33) and the capability of calculating α by differentiation with respect to q, which we now have, make possible the presentation of the scaling properties of dynamical fluctuations in terms of the multifractal spectrum $f(\alpha)$.

It is not our purpose here to examine specific dynamical models or experimental data and to extract their multiplicity fluctuation behaviors. However, we can demonstrate the nature of $f(\alpha)$ if we assume that the scaling behavior (33) is true for a set of $P_n(\delta)$ for a range of δ. Let us further assume that among those $P_n(\delta)$, a specific one at some δ_0 is exactly $\mathcal{P}_n^{(1)}$ given in (28). Then we have

$$\varphi(q) = c \ln F(q) + c_1(q) , \tag{37}$$

where $c = (-\ln\delta_0)^{-1}$ and $c_1(q)$ is some function of q independent of δ_0 arising from the proportionality factor in (33). Scaling behavior means that $\varphi(q)$ is unchanged, as δ is varied from δ_0. The major part of the q dependence of $\varphi(q)$ derives from that of $F(q)$, which we know from Fig. 6. Apart from the unknown constant c and the unknown function $c_1(q)$ in this example, we can determine $f(\alpha)$ from $F(q)$ by varying q parametrically. For illustrative purpose, let us assume that $c_1(q) = 0$ so that using (34)–(37) and the result of our calculated $F(q)$ pertaining to $\mathcal{P}_n^{(1)}$, we can determine $f(\alpha)$. In Fig. 8 we show the result for four possible values of c. We stress that in a model or data analysis c is not a variable, $\varphi(q)$ is determined from the log-log plots when there is scaling. Figure 8 merely illustrates the possible form of $f(\alpha)$, if $\varphi(q)$ happens to coincide with the result of analyzing a particular $P_n = \mathcal{P}_n^{(1)}$ with a specific c in (37) and with $c_1(q) = 0$. The dashed line indicates where $f(\alpha) = \alpha$, and is tangent to each of the $f(\alpha)$ curves at $q = 1$. The range of q covered by $f(\alpha)$ in Fig. 8 is, depending on c, roughly $-2 \le q \le 4$, with the $q = 0$ point always occurring at the peak of the $f(\alpha)$ curve. The multifractal dimension D_q is [5,16]

$$D_q = \tau(q)/(q-1) , \tag{38}$$

which is related to α by

$$D_0 = f(\alpha_0), \quad D_1 = \alpha_1 , \tag{39}$$

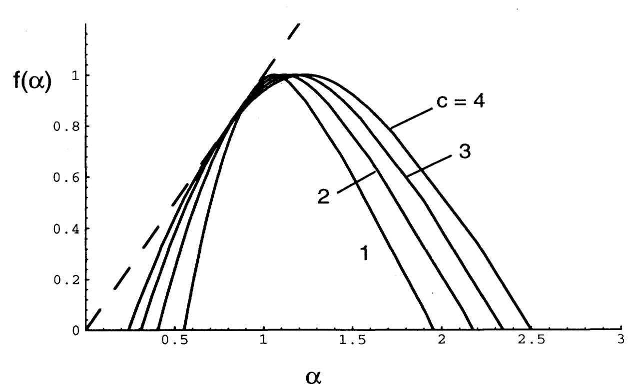

FIG. 8. Multifractal spectra $f(\alpha)$ for four values of c (see text), if the input $\mathcal{P}_N^{(1)}$ belongs to a class of scaling distributions. The dashed line is for $f(\alpha) = \alpha$.

where α_q is the value of α at q. Thus α_0 is where $f(\alpha)$ is maximum, and α_1 is where $f(\alpha_1) = \alpha_1$. The multifractal spectrum $f(\alpha)$ is the most elegant way of displaying the scaling properties of dynamical fluctuation. Reduced to the bare minimum, two parameters can be used to characterize $f(\alpha)$, viz. α_0 and α_1, the location of the peak and a measure of the width, respectively.

In many multiparticle production processes the scaling behavior (33) is not valid over an extended range of δ. The multifractal analysis described above cannot be applied then. However, it has been found phenomenologically [17–19] as well as theoretically [13,20], not only in hadronic and nuclear collisions, but also in quantum optics [14], that F_q satisfies a different scaling law

$$F_q \propto F_2^{\beta_q} \; . \tag{40}$$

Let us assume that this behavior can be established for continuous q so that the function $\beta(q)$ can be determined for a range of q values both positive and negative. Then it is possible to define formally another spectrum, call it $g(\alpha)$, in exact analogy to (34)–(36), but without the geometrical implication of multifractality. Thus we define

$$\sigma(q) = q - 1 - \beta(q) \; , \tag{41}$$

$$g(\alpha) = g\alpha - \sigma(q) \; , \tag{42}$$

$$\alpha = d\sigma(q)/dq \; . \tag{43}$$

The only input into this scheme of description is $\beta(q)$, which is

$$\beta(q) = \ln F(q)/\ln F(2) + b(q) \; , \tag{44}$$

where $b(q)$ is the log of the proportionality factor in (40). Mathematically, $\sigma(q)$ and $g(\alpha)$ correspond to $\tau(q)$ and $f(\alpha)$ if we set $c = 1/\ln F(2)$, but physically (33) need not be true, rendering $\varphi(q)$ meaningless, while (40) can well be true (no exception having been found so far). Reference [13] gives an explicit example of (40) being valid for a problem that does not have (33).

In the example where $\mathcal{P}_n^{(1)}$ is considered, let us assume that it belongs to the type of physical problem for which (40) is valid. Then the function $F(q)$ obtained is sufficient to determine $g(\alpha)$, assuming $b(q) = 0$. The result is shown in Fig. 9(a). Since $F(2) = 1.14$, $g(\alpha)$ corresponds to $f(\alpha)$ in Fig. 8 with $c = 7.64$. In Fig. 9(a), the peak occurs at $\alpha_0 = 1.45$ while the tangent point is at $\alpha_1 = 0.52$. If, on the other hand, $\mathcal{P}_n^{(2)}$ is used as an example that has a scaling behavior (40), totally unrelated to $\mathcal{P}_n^{(1)}$, then the corresponding spectrum $g(\alpha)$ is as shown in Fig. 9(b). Note that in this case the maximum α is 2.15 corresponding to $q = -0.24$. Our continuation to lower value of q has led to a sudden downturn of $F(q)$ around $q = -0.4$, exhibited in Fig. 7(b). That causes a drastic change in the derivative in (43) at around $q = -0.24$ which in turn gives rise to an irregular behavior in $g(\alpha)$ at $\alpha = 2.15$. Thus the nature of $\mathcal{P}_n^{(2)}$ prevents the use of $F(q)$ for $q < -0.24$, thereby setting an upper bound to how far to the right the spectrum $g(\alpha)$ can be developed. In that figure $\alpha_0 = 1.76$ and $\alpha_1 = 0.41$, quite different from the corresponding values in Fig. 9(a). These two figures are sufficient to indicate that $\mathcal{P}_n^{(1)}$ and $\mathcal{P}_n^{(2)}$ cannot belong to the same class of F-scaling factorial moments.

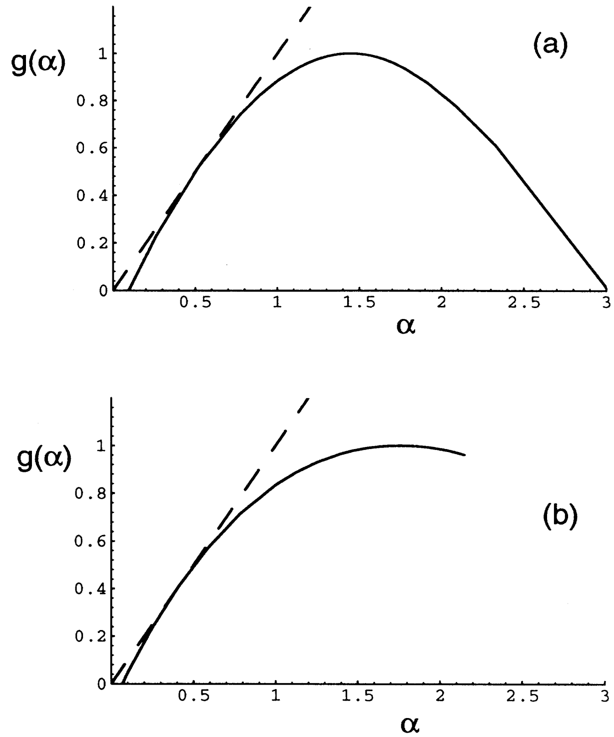

FIG. 9. Spectrum function $g(\alpha)$ is (a) $\mathcal{P}_n^{(1)}$ and (b) $\mathcal{P}_n^{(2)}$ belong to separate classes of self-similar distributions satisfying F scaling (3.9).

In summary, $g(\alpha)$ is a representation of the characteristics of the F-scaling behavior, (40), of $F(q)$, and may be a generally useful description of all multiparticle production processes.

VII. CONCLUSION

We have presented a way to determine $F(q)$ for continuous q such that it is 1 for all q if the input distribution is Poissonian, i.e., the statistical fluctuation is filtered out. The range of q into which $F(q)$ can be continued depends on the nature of P_n. Generally speaking, the low n part of P_n is characterized by the negative q region of $F(q)$. Thus the study of the scaling behavior of multiplicity fluctuations can now be extended to dips, gaps, and voids. All existing data that have been put to intermittency analysis at positive integer q should be reanalyzed for continuous q. Similarly, such reanalysis should be done for all models and Monte Carlo (MC) codes. Thus the confrontation between theory and experiment can now be extended to a significant portion of the real line of q, as compared to the previous situation where it has been done for only a few isolated points at the integer values. For comparison, the study of Bose-Einstein correlation is focused on only one point: $q = 2$.

If the dynamics of particle production is self-similar so that $F(q)$ exhibits a power-law dependence on the resolution scale δ, then the intermittency index $\varphi(q)$ can be determined as a continuous function of q. It then follows that the multifractal spectrum $f(\alpha)$ can be derived without any ambiguity or need for correction to eliminate statistical contamination. On the other hand, if there is no power-law dependence on δ, but there is F scaling, i.e., $F_q \propto F_2^{\beta_q}$, which is more commonly observed, then the knowledge of $\beta(q)$ is sufficient to determine the spectrum $g(\alpha)$ that gives an excellent description of the self-similar behavior of the dynamics of fluctuations.

For the purpose of providing a convenient outline of the procedure to determine $F(q)$, $f(\alpha)$, and $g(\alpha)$, we summarize here the steps needed to do the analysis.

(1) Starting with the input P_n, $n = 0, \ldots, N$, determine x and k from (23) and (24), and then x_j and k_j from (25)–(27) with $\Delta = 0.5$. When x is very small, use (30) instead of (26).

(2) Using (12), set up $N + 1$ linear algebraic equations, (11), with $P_n^{\mathrm{NB}}(j)$ as the matrix and P_n as the input vector. Solve for a_j, $j = 0, \ldots, N$. (The use of MATHEMATICA has been found to be convenient.)

(3) Use (21) to calculate $F(q)$ for a range of real q.

(4) If the input $P_n(\delta)$ is known for a range of δ, determine $f(q)$ as a function of δ and examine the validities of (33) and (40) over that range of δ.

(5) If (33) is valid for a subrange of δ, then from $\varphi(q)$ and (34)–(36) determine $f(\alpha)$.

(6) If (33) is invalid but (40) is valid, then from $\beta(q)$ and (41)–(43) determine $g(\alpha)$.

(7) Compare theory and experiment at any of the three levels: $F(q)$, $f(\alpha)$, or $g(\alpha)$.

ACKNOWLEDGMENTS

I am grateful to I. M. Dremin and J.-L. Meunier for helpful discussions. This work was supported, in part, by the U.S. Department of Energy under Grant No. DE-FG06-91ER40637.

[1] A. Białas and R. Peschanski, Nucl. Phys. **B273**, 703 (1986); **B308**, 867 (1988).
[2] *Soft Physics and Fluctuations*, edited by A. Białas, K. Fiałkowski, K. Zalewski, and R. C. Hwa (World Scientific, Singapore, 1994).
[3] NA22 Collaboration, N. Agababyan *et al.*, Z. Phys. C **59**, 405 (1993); UA1 Collaboration, N. Neumeister, *et al.*, Phys. Lett. B **275**, 186 (1992); DELPHI Collaboration, P. Abreu *et al.*, Z. Phys. C **63**, 17 (1994).
[4] NA22 Collaboration, N. Agababyan *et al.*, Phys. Lett. B **332**, 458 (1994); W. Kittel, *Proceedings of the 23rd International Symposium on Multiparticle Dynamics*, Aspen, 1993, edited by M. M. Block and A. R. White (World Scientific, Singapore, 1994), p. 251.
[5] R. C. Hwa, Phys. Rev. D **41**, 1456 (1990); C. B. Chiu and R. C. Hwa, *ibid.* **43**, 100 (1991); R. C. Hwa, in *Quark-Gluon Plasma*, edited by R. C. Hwa (World Scientific, Singapore, 1990).
[6] R. C. Hwa and J. Pan, Phys. Rev. D **45**, 1476 (1992); I. Derado, R. C. Hwa, G. Jancso, and N. Schmitz, Phys. Lett. B **283**, 151 (1992).
[7] C. B. Chiu, K. Fiałkowski, and R. C. Hwa, Mod. Phys. Lett. A **5**, 2651 (1990).
[8] K. B. Oldham and J. Spanier, *The Fractional Calculus* (Academic, New York, 1974).
[9] M. Blazek, Phys. Lett. B **247**, 576 (1990).
[10] P. Duclos and J.-L. Meunier, Z. Phys. C **64**, 295 (1994).
[11] I. M. Dremin, Pis'ma Eksp. Teor. Fiz. Zh. **59**, 561 (1994) [JETP Lett. **59**, 585 (1994)]; Usp. Fiz. Nauk **164**, 785 (1994).
[12] P. Carruthers and C. C. Shih, Int. J. Mod. Phys. A **2**, 1447 (1987).
[13] R. C. Hwa and M. T. Nazirov, Phys. Rev. Lett. **69**, 741 (1992).
[14] M. R. Young, Y. Qu, S. Singh, and R. C. Hwa, Opt. Commun. **105**, 325 (1994).
[15] J. Feder, *Fractals* (Plenum, New York, 1988).
[16] H. G. E. Hentschel and I. Procaccia, Physica D **8**, 435 (1983).
[17] W. Ochs, Phys. Lett. B **247**, 101 (1990); Z. Phys. C **50**, 339 (1991).
[18] M. Charlet, Ph.D. thesis, University of Nijmegen, 1994; P. Côté, University of Ottawa report, 1994 (unpublished).
[19] J. Pan and R. C. Hwa, Phys. Rev. D **48**, 168 (1993).
[20] R. C. Hwa, Phys. Rev. D **47**, 2773 (1993); Phys. Rev. C **50**, 383 (1994).